

4. T. Nakamura and G. H. Gold, *Nature* **325**, 442 (1987).
5. D. T. Jones and R. R. Reed, *Science* **244**, 790 (1989).
6. R. R. Reed, unpublished data.
7. E. Pfeuffer, S. Mollner, D. Lancet, T. Pfeuffer, *J. Biol. Chem.* **264**, 18803 (1989).
8. J. Krupinski *et al.*, *Science* **244**, 1558 (1989).
9. Oligonucleotide 31C, a nondegenerate 50-nucleotide probe derived from a tryptic fragment of the bovine brain type I adenylyl cyclase was used as described (8). Recombinant phage (200,000) from a rat olfactory oligo(dT)-primed  $\lambda$ gt10 library were screened (28).
10. Low stringency wash conditions: twice for 20 min in 2 $\times$  SSC (standard saline citrate) at 55°C.
11. The complete cDNA of the rat type III adenylyl cyclase was obtained by ligation of two clones. Clone pROSC10-4 (nucleotides -366 to +3183) and clone pROSC6-4 (nucleotides 465 to 4167) were fused at an overlapping Bst EII site at nucleotide 3038 to generate the complete pROSC6+10 construct.
12. M. Kozak, *Nucleic Acids Res.* **15**, 8125 (1987).
13. Other potential sites for N-glycosylation that are predicted to reside on the extracellular face of the type III protein are located at amino acid residues 158 and 827. Additional N-linked glycosylation consensus sequences exist in the large putative intracellular domains, which are similar to the catalytic domains of yeast adenylyl cyclase.
14. T. Kataoka, D. Brock, M. Wigler, *Cell* **43**, 493 (1985); P. Masson, G. Lenzen, J. M. Jacquemin, A. Danchin, *Curr. Genet.* **10**, 343 (1986); M. S. Marshall, J. B. Gibbs, E. M. Scolnick, I. S. Sigal, *Mol. Cell. Biol.* **8**, 52 (1988); J. Field *et al.*, *Science* **247**, 464 (1990).
15. G. A. M. Graziadei and P. P. C. Graziadei, *J. Neurocytol.* **8**, 197 (1979).
16. HAB-1 peptide, H<sub>2</sub>N-YPNGSSVTLPHQVVDNP-COOH, was coupled to bovine serum albumin carrier with glutaraldehyde (32) and used to generate polyclonal antisera in rabbit. This peptide sequence is found at the COOH-terminus of type III adenylyl cyclase, and is not found in any other sequenced adenylyl cyclases.
17. B. Menco, personal communication.
18. C. M. Gorman, D. R. Gies, G. McCray, *DNA and Protein Engineering Techniques* **2**, 3 (1990); D. B. Pritchett *et al.*, *Science* **242**, 1306 (1988).
19. K. B. Seamon, W. Padgett, J. W. Daly, *Proc. Natl. Acad. Sci. U.S.A.* **78**, 3363 (1981).
20. D. T. Jones, S. B. Masters, H. R. Bourne, R. R. Reed, *J. Biol. Chem.* **265**, 2671 (1990).
21. The basal activity for the type I cDNA-transfected 293 cells appeared to be G protein independent. This activity was not reduced with the addition of  $\beta$ -thioguanosine diphosphate (100  $\mu$ M) to the assay mixture (H. Bakalyar, unpublished data).
22. J. Kyte and R. F. Doolittle, *J. Mol. Biol.* **157**, 105 (1982).
23. The activity of the PNGaseF preparation was such that 1  $\mu$ l will completely cleave the N-linked sugars from 100  $\mu$ g of ovalbumin in 60 min at 37°C.
24. U. K. Laemmli, *Nature* **227**, 680 (1970).
25. C. D. Rhein and R. H. Cagan, *Proc. Natl. Acad. Sci. U.S.A.* **77**, 4412 (1980).
26. Antigen purification of sera was performed as described (32). HAB-1 peptide was coupled to Affigel-10 matrix (Bio-Rad) by adding peptide (10 mg) in 10 ml of 0.5 M NaCl and 0.1 M NaHCO<sub>3</sub> to 3 ml of Affigel-10 slurry that had been washed with 1 mM HCl. Resin was incubated on a rotator at room temperature for 30 min. Ethanolamine (1 ml of a 1 M solution) was added and the mixture incubated for 5 min. The peptide-coupled beads were washed on sintered glass and stored at 4°C in 50 mM sodium phosphate (pH 7.0) and 0.1% sodium azide.
27. Samples were treated with glyoxal and separated on a 1% agarose gel as described (28). The fractionated material was transferred to nitrocellulose and prehybridized at 42°C in 50% formamide, 6 $\times$  SSPE (saline, sodium phosphate, EDTA), 5 $\times$  Denhardt's solution, 0.1% SDS, and single-stranded DNA (100  $\mu$ g/ml). The Eco RI fragment representing the full-length type III cDNA was labeled with <sup>32</sup>P and hybridized to the immobilized RNA samples for 48 hours at 42°C. Filters were washed once for 15 min in 1 $\times$  SSC and 0.1% SDS at 25°C, and then twice for 20 min in 1 $\times$  SSC and 0.1% SDS at 65°C.
28. D. T. Jones and R. R. Reed, *J. Biol. Chem.* **262**, 14241 (1987).
29. The complete pROSC6+10 cDNA coding region was cloned into the polylinker site of pCIS (18). Neomycin-resistant stable lines were produced by introduction (30) of pSVneo (0.5  $\mu$ g) and adenylyl cyclase type I or type III cDNA expression plasmids (5  $\mu$ g) or the pCIS vector control into 100-mm culture dishes that contained human kidney 293 cells at ~50% confluency. After 24 hours, G418 (500  $\mu$ g/ml) was added in Dulbecco's modified Eagle's medium containing 10% fetal bovine serum, penicillin (100 U/ml), and streptomycin (100  $\mu$ g/ml). After ~3 weeks, viable clones were transferred to individual dishes and expanded. Adenylyl cyclase assays were performed on each of the clonal cell lines. Forskolin-stimulated activity revealed that one line expressed the type I enzyme and four lines expressed the type III enzyme. Five G418-resistant lines were characterized from transfections with the pSVneo and the pCIS control vectors.
30. P. J. Southern and P. Berg, *J. Mol. Applied Genet.* **1**, 327 (1982).
31. Y. Salomon, in *Advances in Cyclic Nucleotide Research*, G. Brooker, P. Greengard, G. A. Robison, Eds. (Raven Press, NY, 1979), vol. 10, pp. 35-55.
32. E. Harlow and D. Lane, *Antibodies: A Laboratory Manual* (Cold Spring Harbor Laboratory, Cold Spring Harbor, NY, 1988).
33. We thank our colleagues for helpful discussions; P. G. Feinstein for valuable contributions; HHMI-JHU Biopolymer Facility for synthetic oligonucleotides and oligopeptide; G. Hart for PNGaseF; and Genentech for the mammalian expression vector. Supported by NIH grant 5T32CA09339 (to H.A.B.).

5 June 1990; accepted 21 August 1990

## Isotope-Edited NMR of Cyclosporin A Bound to Cyclophilin: Evidence for a *Trans* 9,10 Amide Bond

S. W. FESIK,\* R. T. GAMPE, JR., T. F. HOLZMAN, D. A. EGAN, R. EDALJI, J. R. LULY, R. SIMMER, R. HELFRICH, V. KISHORE, D. H. RICH

The binding of a <sup>13</sup>C-labeled cyclosporin A (CsA) analog to cyclophilin (peptidyl prolyl isomerase) was examined by means of isotope-edited nuclear magnetic resonance (NMR) techniques. A *trans* 9,10 peptide bond was adopted when CsA was bound to cyclophilin, in contrast to the *cis* 9,10 peptide bond found in the crystalline and solution conformations of CsA. Furthermore, nuclear Overhauser effects (NOEs) were observed between the  $\zeta_3$  and  $\epsilon_3$  protons of the methyleucine (MeLeu) residue at position 9 of CsA and tryptophan<sup>121</sup> (Trp<sup>121</sup>) and phenylalanine (Phe) protons of cyclophilin, suggesting that the MeLeu<sup>9</sup> residue of CsA interacts with cyclophilin. These results illustrate the power of isotope-edited NMR techniques for rapidly providing useful information about the conformations and active site environment of inhibitors bound to their target enzymes.

CYCLOSPORIN A (CsA) IS A CYCLIC undecapeptide (Fig. 1) that is widely used as an immunosuppressive agent in organ transplantation (1). Although its precise mechanism of action is unknown, the immunosuppressive activity of CsA may be linked to its affinity for the protein cyclophilin (molecular mass ~17.8 kD), because the binding to cyclophilin appears to correlate with the relative immunosuppressive activities of CsA analogs (2-4). Recently, cyclophilin was shown (5, 6) to have the same amino acid sequence as peptidyl prolyl isomerase, an enzyme that catalyzes the *cis-trans* isomerization of Xaa-proline peptide bonds (where Xaa is any amino acid). Cyclosporin A was found to be

a potent inhibitor of this enzyme, suggesting that some of the biological effects of CsA (7) may be mediated by blocking the enzymatic activity of cyclophilin (8, 9).

In order to aid in the design of CsA analogs with reduced toxicity and potentially greater clinical utility, structural information on the binding of CsA to cyclophilin is desired. To date, however, only the conformation of CsA by itself has been determined in the crystalline state by x-ray crystallography and in apolar solvents by NMR spectroscopy (10). In three different crystal forms of CsA involving different intermolecular contacts and in two different solvent systems (10, 11), CsA was found to adopt an antiparallel  $\beta$ -pleated sheet consisting of residues 11  $\rightarrow$  7 with a type-II'  $\beta$ -turn at residues 2  $\rightarrow$  5. The remaining residues (8 to 10) form a loop defined by a *cis* peptide bond between MeLeu residues 9 and 10. The only differences in the crystal and solution conformations are in the orientation of the 1-MeBmt [(4*R*)-*N*-methyl-4-butenyl-4-

S. W. Fesik, R. T. Gampe, Jr., T. F. Holzman, D. A. Egan, R. Edalji, J. R. Luly, R. Simmer, R. Helfrich, Pharmaceutical Discovery Division, Abbott Laboratories, Abbott Park, IL 60064.  
V. Kishore and D. H. Rich, School of Pharmacy and Department of Chemistry, University of Wisconsin-Madison, Madison, WI 53706.

\*To whom correspondence should be addressed.

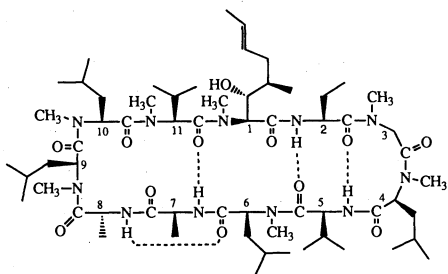


Fig. 1. Structure of cyclosporin A.

methylthreonine] and MeLeu<sup>10</sup> side chains (10). These experimentally determined three-dimensional structures of CsA have been used to predict the bioactive CsA conformation with molecular mechanics calculations (proposed to be similar to the x-ray crystal structure) (12), to rationalize structure-activity relations (3, 7, 12–15), to design conformationally restricted CsA analogs (16), and to interpret the binding specificity of antibodies (11).

In this report we describe NMR studies on the binding of [<sup>13</sup>C]CsA to cyclophilin that provide structural information about the conformation and active-site environment of CsA when it is bound to this enzyme. To simplify the complicated proton NMR spectrum of the complex, we conducted isotope-edited proton NMR experiments (17, 18) with a CsA analog, [U-<sup>13</sup>C-MeLeu<sup>9,10</sup>]CsA, in which the MeLeu residues in the 9 and 10 positions were uniformly labeled (>95%) with <sup>13</sup>C (19). As illustrated in this study, these techniques (17, 18), along with recently developed complementary methods (20) for assigning the NMR resonances of the bound ligand, are extremely useful for rapidly obtaining detailed structural information on enzyme-inhibitor complexes.

An isotope-edited two-dimensional (2-D) NOE spectrum of [U-<sup>13</sup>C-MeLeu<sup>9,10</sup>]CsA bound to recombinant human cyclophilin is shown in Fig. 2 (21). In the  $\omega_1$  dimension, only those protons attached to the <sup>13</sup>C-labeled nuclei of CsA are detected. In the  $\omega_2$  dimension, NOE cross-peaks between these "labeled" protons and other nearby protons of CsA and cyclophilin are observed. The proton NMR assignments of the [<sup>13</sup>C]CsA residues are given to the left of the spectrum. These assignments were made from an analysis of <sup>1</sup>H-<sup>13</sup>C correlation experiments. In the heteronuclear multiple quantum correlation (HMQC) spectrum (22), shown in Fig. 3A, the  $\alpha$ - and methyl protons were readily identified from their chemical shifts and relative signal intensities, and the  $\beta$ - and  $\gamma$ -signals of both MeLeu residues were distinguished by their different <sup>13</sup>C chemical shifts (23).

The NMR signals that correspond to the nuclei belonging to the same spin system were identified by a recently developed NMR experiment (20) in which <sup>13</sup>C-<sup>13</sup>C isotropic mixing was followed by <sup>13</sup>C-<sup>1</sup>H magnetization transfer. Because of the large magnitude of <sup>13</sup>C-<sup>13</sup>C and <sup>13</sup>C-<sup>1</sup>H one-bond *J* couplings ( $J_{CC} \geq 35$  Hz and  $J_{CH} \geq 125$  Hz), coherence transfers can be effected in a short period of time in this experiment, allowing the scalar (through-bond) coupled protons and carbons to be identified even in large molecules with broad NMR signals (20). Correlations were identified between the  $\beta$ ,  $\gamma$ ,  $\delta$ , and  $\delta'$  carbons and the  $\delta$  methyl protons for both the MeLeu<sup>9</sup> and MeLeu<sup>10</sup> spin systems (vertical lines,  $\delta$ ), as shown in Fig. 3B. In addition, C <sup>$\delta$</sup> , C <sup>$\delta'$</sup> , C <sup>$\gamma$</sup> -H <sup>$\gamma$</sup>  (Fig. 3B,  $\gamma$ ) and C <sup>$\beta$</sup> , C <sup>$\alpha$</sup> -H <sup>$\alpha$</sup>  (Fig. 3B,  $\alpha$ ) correlations were observed. The NCH<sub>3</sub> protons and carbonyl carbons were assigned from a heteronuclear multiple-

bond correlation (HMBC) experiment (24) in which the NCH<sub>3</sub> protons of MeLeu<sup>10</sup> and the carbonyl carbon of MeLeu<sup>9</sup> were correlated. The <sup>13</sup>C chemical shifts of the MeLeu<sup>9</sup> (171.3 ppm) and MeLeu<sup>10</sup> (173.2 ppm) carbonyls that were observed are typical for amides (23) and are inconsistent with a tetrahedral adduct (6) at this site.

We interpreted the isotope-edited NOE data using the proton NMR assignments of the MeLeu<sup>9</sup> and MeLeu<sup>10</sup> CsA residues. The intense NOE observed between the MeLeu<sup>10</sup> NCH<sub>3</sub> and the MeLeu<sup>9</sup> H <sup>$\alpha$</sup>  of CsA (Fig. 2) is characteristic of an extended conformation of the peptide backbone with a *trans* 9,10 amide bond. A *cis* peptide bond would be characterized by an NOE between the  $\alpha$  protons of adjacent amino acids (25). However, no NOE was observed between the 9 and 10  $\alpha$  protons (Fig. 2). The observation of a *trans* 9,10 peptide bond indicates that the conformation of CsA

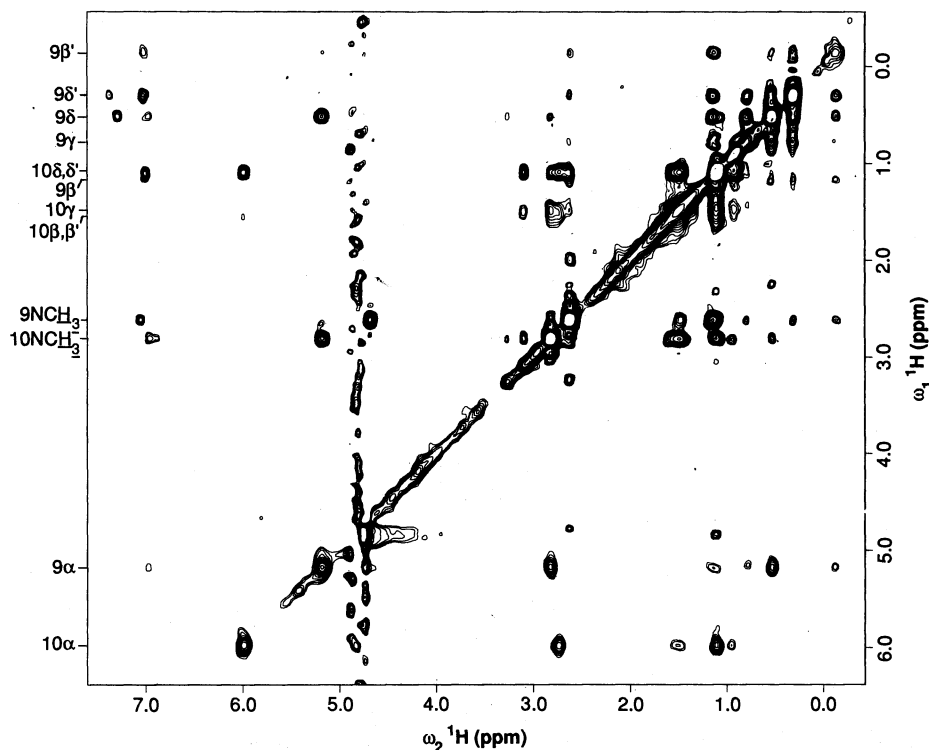


Fig. 2. Contour plot of an isotope-edited 2-D NOE spectrum of a 1.3 mM solution of [U-<sup>13</sup>C-MeLeu<sup>9,10</sup>]CsA and recombinant human cyclophilin (1/1). We prepared the complex as recently described (27) by gently mixing a 1.5 M excess of [U-<sup>13</sup>C<sup>9,10</sup>]CsA and cyclophilin in a <sup>2</sup>H<sub>2</sub>O solution containing 100 mM NaCl, 50 mM phosphate buffer (pH 6.5), and 2 mM deuterated dithiothreitol at 6°C for 12 hours under argon, and then removing the excess CsA by centrifugation. The cyclophilin was isolated from *Escherichia coli* that overexpressed human cyclophilin (28). The  $\omega_1$ -filtered 2-D NOE data were acquired at 20°C on a Bruker AM500 NMR spectrometer equipped with an inverse probe using the pulse sequence: 90(<sup>1</sup>H)- $\tau$ -180(<sup>1</sup>H), 90(<sup>13</sup>C), 90(<sup>13</sup>C)- $\tau$ -t<sub>1</sub>-90(<sup>1</sup>H)- $\tau_m$ -90(<sup>1</sup>H)-acquire(t<sub>2</sub>) in which the phase of the second 90° <sup>13</sup>C pulse and receiver are inverted on alternate scans. We applied <sup>13</sup>C-decoupling during t<sub>1</sub> and t<sub>2</sub> with a GARP pulse sequence (29). A total of 128 scans were acquired for 2 by 150 t<sub>1</sub> increments with delays of  $\tau = 3.3$  ms,  $\tau_m = 70$  ms, and a recycle delay of 1.2 s. The residual solvent signal was suppressed with low-power irradiation during  $\tau_m$  and delay between scans. The NMR data were processed on a Vax 8350 with a slave Mini-MAP array processor (CSP, Inc.) by using the Fourier transform NMR program of D. Hare and software written at Abbott Laboratories. Gaussian and cosine window functions were applied in t<sub>2</sub> and t<sub>1</sub>, respectively, before Fourier transformation. Assignments of the MeLeu<sup>9</sup> and MeLeu<sup>10</sup> protons of CsA are given to the left of the spectrum. (GARP, globally optimized alternating-phase rectangular pulses.)

when bound to cyclophilin is markedly different from the reported (10) crystalline and solution conformation of CsA, which contains a *cis* 9,10 amide bond. A *trans* 9,10 peptide bond may be accommodated within the macrocyclic ring of CsA by forming a *cis* peptide bond elsewhere in the molecule. However, recent NMR studies (26) of uniformly labeled [<sup>13</sup>C]CsA bound to cyclophilin indicate that only *trans* CsA peptide bonds are present.

In addition to providing information about the enzyme-bound inhibitor conformation, these NMR experiments provide structural information about the enzyme binding site by means of the NOEs between "labeled" protons of CsA and cyclophilin. For example, NOEs were observed between several protons of the MeLeu<sup>9</sup> residue of CsA and aromatic protons of cyclophilin (Fig. 2), which is consistent with the upfield shifts observed for the MeLeu<sup>9</sup> protons of CsA when bound to cyclophilin. In particular, NOEs were observed (Fig. 2) between the δ'CH<sub>3</sub> protons of MeLeu<sup>9</sup> and aromatic portions of cyclophilin that resonate at 7.38

and 7.02 ppm, which correspond (27) to the ζ<sub>3</sub> and ε<sub>3</sub> protons of cyclophilin's only Trp residue. In an isotope-edited 2-D NOE spectrum acquired with a longer mixing time (140 ms), an additional NOE between the MeLeu<sup>9</sup> δ'CH<sub>3</sub> and the Trp<sup>121</sup> η proton (7.50 ppm) was observed.

NOEs were also detected between the MeLeu<sup>9</sup> δCH<sub>3</sub> protons of CsA and cyclophilin protons resonating at 7.29 and 7.01 ppm, and at 6.64 ppm in a 2-D NOE data set acquired at a longer mixing time (200 ms); these are consistent with the chemical shifts of cyclophilin Phe protons (27) (the identification of which Phe residues awaits the sequence-specific proton NMR assignments). Although previous studies based on structure-activity relations have inferred that only CsA residues 1, 2, 3, 10, and 11 are involved in binding to cyclophilin (3), it appears from the NOE data that the MeLeu<sup>9</sup> residue of CsA is in close proximity to the ζ<sub>3</sub> and ε<sub>3</sub> protons of Trp<sup>121</sup> (Trp<sup>120</sup> in bovine cyclophilin) and a Phe residue of cyclophilin. The observed cyclophilin binding affinity and immunosuppressive activity

displayed by 9-substituted cyclosporins may be explained by a lack of selectivity of the MeLeu<sup>9</sup> binding pocket of cyclophilin, which could allow binding of a variety of structurally different 9-substituted CsA analogs.

The formation of a *trans* amide bond between MeLeu<sup>9</sup> and MeLeu<sup>10</sup> when CsA is bound to cyclophilin suggests that the bioactive conformation of CsA is very different from the crystalline (9) and solution conformations of CsA, in which this amide bond is *cis*. Furthermore, although it has been proposed (3) that the MeLeu<sup>9</sup> residue is not involved in the interaction of CsA with cyclophilin, we have identified NOEs between the MeLeu<sup>9</sup> residue of CsA and Trp<sup>121</sup> and Phe protons of cyclophilin. These results suggest that the interpretation of structure-activity relations or the design of CsA analogs based on the previously reported crystalline or solution conformation of CsA must be treated with caution, and they highlight the importance of obtaining structural information on drug molecules bound to their target sites.

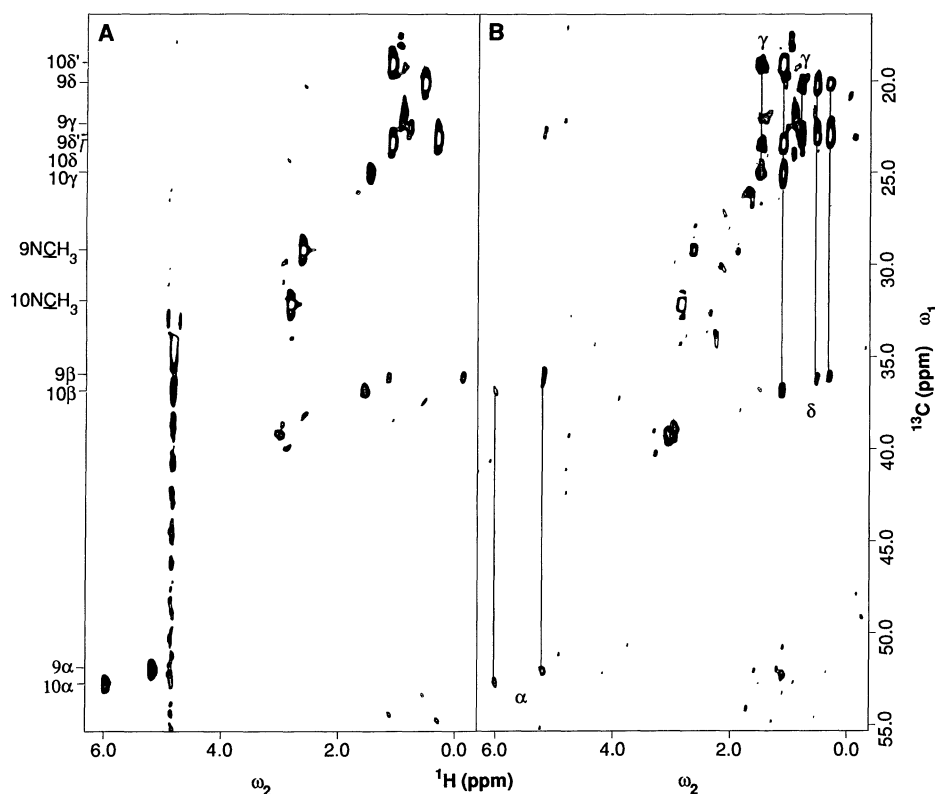


**Fig. 3.** (A) <sup>1</sup>H-<sup>13</sup>C HMQC and (B) <sup>13</sup>C TOCSY-REVINEPT spectrum (20) of the CsA-cyclophilin complex described in the legend to Fig. 2. The <sup>13</sup>C TOCSY-REVINEPT experiment was conducted as previously described (20) except that a DIPSI-2 pulse sequence (30) was used to cover a wider bandwidth during the 12-ms isotropic mixing period. A BSV3 continuous wave amplifier connected to the observe channel was used for the hard 90° <sup>13</sup>C pulses (36 μs) and DIPSI-2 mixing scheme. An additional BSV3 amplifier driven from a PTS synthesizer interfaced to a GARP box (Tschudin Associates) was used for <sup>13</sup>C-decoupling during the acquisition period. The <sup>13</sup>C NMR assignments are given to the left of the spectra. (TOCSY-REVINEPT, total correlation spectroscopy—reverse insensitive nucleus enhancement by polarization transfer; PTS, programmed test sources; DIPSI, decoupling in the presence of scalar interactions.)

#### REFERENCES AND NOTES

1. C. R. Stiller and P. A. Keown, in *Progress in Transplantation*, P. J. Morris and N. L. Tilney, Eds. (Churchill-Livingstone, New York, 1984), vol. 1, pp. 11–45.
2. R. E. Handschumacher, M. W. Harding, J. Rice, R. J. Drugge, D. W. Speicher, *Science* **226**, 544 (1984).
3. V. F. J. Quesniaux *et al.*, *Eur. J. Immunol.* **17**, 1359 (1987).
4. For an exception, see D. H. Rich *et al.*, in *Peptides: Chemistry, Structure and Biology*, J. E. Rivier and G. R. Marshall, Eds. (ESCOM Science, Leiden, the Netherlands, 1990), pp. 49–52.
5. N. Takahashi, T. Hayano, M. Suzuki, *Nature* **337**, 473 (1989).
6. G. Fischer, B. Wittman-Liebold, K. Lang, T. Kiefhaber, F. X. Schmid, *ibid.*, p. 476.
7. R. M. Wenger, T. G. Payne, M. H. Schreier, *Prog. Clin. Biochem. Med.* **3**, 157 (1986).
8. J. J. Sierkierka, S. H. Y. Hung, M. Poe, C. S. Lin, N. H. Sigal, *Nature* **341**, 755 (1989).
9. M. W. Harding, A. Galat, D. E. Uehling, S. L. Schreiber, *ibid.*, p. 758.
10. H.-R. Loosli *et al.*, *Helv. Chim. Acta* **68**, 682 (1985).
11. V. F. J. Quesniaux, R. M. Wenger, D. Schmitter, M. H. V. Van Regenmortel, *Int. J. Pep. Protein Res.* **31**, 173 (1988).
12. K. E. Miller and D. H. Rich, *J. Am. Chem. Soc.* **111**, 8351 (1989).
13. R. M. Wenger, *Angew. Chem. Int. Ed. Engl.* **24**, 77 (1985).
14. D. H. Rich *et al.*, *J. Med. Chem.* **32**, 1982 (1989).
15. J. D. Aebi *et al.*, *ibid.* **33**, 999 (1990).
16. J. D. Aebi, D. Guillaume, B. E. Dunlap, D. H. Rich, *ibid.* **31**, 1805 (1988).
17. G. Otting, H. Senn, G. Wagner, K. Wuthrich, *J. Magn. Reson.* **70**, 500 (1986).
18. S. W. Fesik, J. R. Luly, J. W. Erickson, C. Abad-Zapatero, *Biochemistry* **27**, 8297 (1988).
19. We prepared CsA uniformly <sup>13</sup>C-labeled at the 9,10 position using the procedures described in (13). [<sup>13</sup>C]Leu (>95%) was obtained from Cambridge Isotopes.
20. S. W. Fesik *et al.*, *J. Am. Chem. Soc.* **112**, 886 (1990).
21. Isotope-edited 2-D NOE spectra were also obtained on [<sup>13</sup>C]CsA bound to bovine cyclophilin isolated

from calf thymus, and the NMR spectra are identical.

22. L. Muller, *J. Am. Chem. Soc.* **101**, 4481 (1979).
23. K. Wüthrich, *NMR of Proteins and Nucleic Acids* (Wiley, New York, 1986).
24. A. Bax and M. F. Summers, *J. Am. Chem. Soc.* **108**, 2093 (1986).
25. K. Wüthrich, M. Billeter, W. Braun, *J. Mol. Biol.* **180**, 715 (1984).
26. S. W. Fesik *et al.*, unpublished data.
27. S. L. Heald, M. W. Harding, R. E. Handschumacher, I. M. Armitage, *Biochemistry* **29**, 4466 (1990). The proton chemical shifts that are reported in this paper are referenced relative to sodium 3-trimethyls-

- ilylpropionate-2,2,3,3- $d_4$  and are 0.05 ppm upfield relative to those given by Heald *et al.*
28. T. F. Holzman *et al.*, unpublished data.
29. A. J. Shaka, P. B. Barker, R. Freeman, *J. Magn. Reson.* **64**, 547 (1985).
30. S. P. Rucker and A. J. Shaka, *Mol. Phys.* **68**, 509 (1989).
31. We thank N. BaMaung for assisting in the preparation of [ $^{13}\text{C}$ ]MeLeu, and T. J. Perun and G. W. Carter for their support and encouragement.

31 May 1990; accepted 31 July 1990

## Detection of Radial Crossbridge Force by Lattice Spacing Changes in Intact Single Muscle Fibers

G. CECCHI, M. A. BAGNI, P. J. GRIFFITHS,\* C. C. ASHLEY, Y. MAEDA

**Time-resolved lattice spacing changes were measured (10-millisecond time resolution) by x-ray diffraction of synchrotron radiation in single intact muscle fibers of the frog *Rana temporaria* undergoing electrically stimulated tension development during application of stretches and releases. Ramp releases, which decreased fiber length at constant speed, caused a lattice expansion. After the ramp, increasing tension during recovery was accompanied by lattice compression. Ramp stretches caused a compression of the lattice. While the fiber was held at a constant length after the stretch, tension decreased and lattice spacing increased. These observations demonstrate the existence of a previously undetected radial component of the force generated by a cycling crossbridge. At sarcomere lengths of 2.05 to 2.2 micrometers, the radial force compresses the myofilament lattice. Hence, the myofilament lattice does not maintain a constant volume during changes in force.**

ACCORDING TO THE MOST WIDELY accepted theory of muscle contraction (1), tension development occurs as a result of the interaction of actin and myosin filaments along radial projections from the myosin filament (crossbridges). These projections contact the actin filament during activation and exert a force directed axially that is responsible for sarcomere shortening. However, this force may also have components directed radially with respect to the axis of the myosin filament. The action of such radial forces on the filament lattice depends on the geometrical arrangement of the components of the attached crossbridge structure. A compression of skinned fibers on entering the rigor state and on calcium activation (2) has been reported, but, until now, no such radial force component has been detected experimentally in intact fibers during electrically stimulated

tension generation (tetanus). We report on time-resolved lattice spacing measurements performed on single intact skeletal muscle fibers of the frog during rapid length changes imposed on the fiber during tetani. Changes in the myofilament lattice during active tension development are consistent with the existence of a radially compressive force on the myofilament lattice associated with crossbridge activity at slack length. These results are inconsistent with constant volume theory and allow testing of particular theories of crossbridge force generation. In particular, they impose important constraints on the geometry of the structural change accompanying tension development by the crossbridge and suggest the importance of accounting for radial forces in current crossbridge theories.

During tetani, single muscle fibers were exposed to x-ray synchrotron radiation, and the equatorial x-ray diffraction pattern of the fiber was recorded. At the tetanus plateau, ramp shortening of a fiber at a velocity sufficient to reduce tension from its isometric level ( $P_0$ ) to  $0.05 P_0$  caused a rapid shift in the position of the equatorial reflections toward the center of the diffraction pattern, which corresponds to an expansion of the myofilament lattice (3) and a partial reversal

of the equatorial intensity changes associated with activation of the muscle toward the relaxed intensity pattern. While force remained low (because of the continuing shortening of the preparation), the lattice remained expanded. When shortening ceased, the fiber recovered tension rapidly to the new plateau level. The recovery of tension was associated with a compression of the lattice. An example of this behavior is shown in Fig. 1A. Although the expansion of the lattice associated with the shortening of the preparation is accompanied by a decrease in sarcomere length, the compression of the lattice during the recovery of tension occurs under virtually isometric conditions (Fig. 1B).

If the activated fiber behaves as a constant volume system as already reported for passive fibers (4), then sarcomere shortening would be expected to result in a lattice expansion, being apparently consistent with the present observation. However, lattice expansion is bigger than expected for constant volume behavior. In fact, calculation of lattice volume from the lattice spacing and the sarcomere length changes shows that a considerable increase in lattice volume occurred during shortening (Fig. 1C). During the subsequent recovery of tension after the release was terminated, the lattice volume returned to a value close to that found before the release.

During a ramp stretch, force increased rapidly at first, after which it stabilized at a new level, and the remainder of the stretch ramp occurred under isotonic conditions (Fig. 2, A and B). Lattice spacing was reduced during the rise of force and underwent reextension after completion of the stretch, during the return of force to the isometric level. By plotting the lattice volume calculated from the sarcomere length signal and the lattice spacing, we found that this behavior cannot be accounted for if constant volume of the lattice is assumed (Fig. 2C).

Our findings show that, during shortening of a fiber at a rate sufficient to reduce force to  $0.05 P_0$ , a lattice expansion occurs. However, the time course of this expansion is more similar to the time course of the fall of force and is not similar to the ramp length change as would be expected from constant volume behavior. During the recovery of tension after completion of a ramp, virtually no change in sarcomere length was observed. Since during this period tension is rising, the expected behavior, according to constant volume constraints, should be a lattice expansion as series compliance is re-extended and the contractile system shortens (5). However, what is actually observed is a compression of the lattice. A similar argu-

G. Cecchi and M. A. Bagni Dipartimento di Scienze Fisiologiche, Università degli studi di Firenze, I-50134 Florence, Italy.

P. J. Griffiths and C. C. Ashley, University Laboratory of Physiology, University of Oxford, OX1 3PT, United Kingdom.

Y. Maeda, European Molecular Biology Laboratory Outstation, Deutsches Elektronen Synchrotron, Hamburg D2000, Federal Republic of Germany.

\*To whom correspondence should be addressed.